Evaluation of machine-tool motion accuracy using a CNC machining centre in micro-milling processes

Elisa VÁZQUEZ[1], Jéssica GOMAR[1], Joaquim CIURANA*[1], and Ciro RODRÍGUEZ[2]

[1]Department of Mechanical Engineering and Industrial Construction, Universitat de Girona, Spain
[2]Center for Innovation in Design and Technology, Tecnológico de Monterrey, Monterrey, Mexico

***Corresponding Author**: quim.ciurana@udg.edu

Abstract

The demand for micro holes, micro-moulds and micro forms continues to grow as high-tech industries demand miniaturized products. Sectors such as aerospace, microelectronics, medicine, and even the automotive sector, are just some examples of enterprises that are taking advantage of micro-manufacturing technologies. Within this framework, the need to adapt the knowledge of macro-scale manufacturing processes to micro-scale is evident. This paper evaluates, through theoretical principles and experimental work, the machine-tool motion accuracy of a medium machining centre specializing in the micro-milling of elliptical cavities on aluminium workpieces. Measurements were taken to evaluate: deviations and/or errors in geometric accuracy, and the geometric quality errors caused by motion control and control software. The results show that, due to the structure and inertia of the machine tool, acceleration and deceleration do indeed affect the accuracy and quality of the micro-part. Furthermore, errors from motion control and/or control software are present because differences in the moving carriages create instabilities.

Keywords: micro-machining, micro-tool, micro-cavities.

1. Introduction

As many high-tech industries are now using miniaturized parts or products the demand for micro holes, micro-moulds and micro forms continues to increase. Aerospace, microelectronics, the medical sector together with the automotive sector, are but some examples of enterprises that are making the most of the micro-manufacturing technologies. Nowadays, the key success factor of these technologies comes from the ability to be flexible and manufacture a complete part in a single machining process. To meet the large scale production needs of mechanical components and micro products, the need to adapt the manufacturing process knowledge from macro-scale to micro-scale is evident.

One of the most significant research subjects in milling processes is in evaluating machine-tool motion accuracy, as this has a noticeable influence on the quality of the final machined part.

One of the first works in this field of research was developed by Weck and Schmidt [1], where they proposed a method using a laser beam and a four quadrant photodiode to evaluate the radial error-motion of a rotating table of a gear hobbing machine. Furthermore, they quantified the parallelism between the rotating axis and a linear guide-way. With the same approach, Zhang et al. [2] developed a displacement method to measure the 21 error components in the geometric error using a laser interferometer. Similar research work found that by measuring the positioning errors along the 15 lines in the machine work zone, a total of 21 geometric error components can be determined [3]. Iwasawa et al. [4] used a laser displacement interferometer and a rotary encoder to measure a much longer range of motion than ordinal circular test methods such as the double ball bar method can. Additionally, the proposed method allows positioning accuracy and other more complex test paths to be evaluated.

Measurement and evaluation of motion errors by the Double Ball Bar (DBB) test is a commonly used method, particularly in dynamic circle path tests. Bryan [5] and Kakino et al. [6] were pioneers in the use of this technique. Lai et al. [7] proposed a mathematical model that diagnoses the nonlinear error source in a guide-way system by measuring the contouring error using a double ball bar. A more robust system was developed by Qiu et al. [8, 9], when they developed a device consisting of a double-bar linkage and two Canon K-1 laser rotary encoders. The experimental results demonstrated that the method and device developed are capable of evaluating most items of motion accuracy in NC machine tools. Similar work used three laser ball bars [10].

Die-manufacturing demands have allowed a measuring method to be developed that consists of a cross grid encoder. This method is widely used in two dimensions, i.e. in an XY, YZ or XZ-plane, because it has the ability to work with any chosen path. Rehsteiner and Weikert [11] used this method to evaluate motion accuracy in machine tools. Du et al. [12] developed a multi-step measuring method for motion accuracy in NC machine tools using a cross grid encoder and based on the kinematic error model of an NC machine tool. However, using these same macro-scale evaluation techniques to appraise machine-tool motion accuracy performance has disadvantages when applied to micro-scale. In the case of double ball bar, measuring range is greater than the scale of the interest. When this method is used, it is not possible to measure the servo induced error in machine tools in small-radius circular test paths. On the other hand, laser interferometer results are significantly dependent on environmental conditions as the laser wave length depends on temperature, humidity, air pressure and air circulation [12].

Kim et al. [13], Monreal and Rodriguez [14] and Schmitz et al. [15], conducted investigations into the contribution of acceleration and deceleration in macro-scale part dimensional errors, while Philip et al. [16], who studied a micro-scale case, proposed a new acceleration-based methodology for micro/meso-scale machine tool performance evaluation. The authors developed two micro/meso-scale machine tool (mMT) prototypes at the University of Illinois in Urbana-Champaign. These were then used as test vehicles for new performance evaluation

methodology. This novel research presents a technique for measuring radial and tilt error motions of ultra-high-speed miniature spindles. The technique was based on measurements of radial motions in two mutually orthogonal directions of a precision artefact using (non-contact) laser Doppler vibrometers [17].

According to Schwenke [18], the main error sources affecting accuracy are kinematic errors, thermo-mechanical errors, loads, dynamic forces and motion control and control software. In the case of thermal-mechanical errors, these are present due to modifications of heat/cold sources in machine tools and therefore to thermal expansion coefficients. Several studies have focussed on this issue [19-21]. The finite stiffness of the structural loop can be a significant influence on the machine's accuracy; which can occur due to the weight and position of, for example, the workpiece or moving carriages of the machine. Schwenke [18] Schellekens et al. and Spaan, reported that these kinds of errors are more important in comparison with kinematic errors. In the case of dynamic forces, the machining forces, measuring forces or forces caused by accelerations or decelerations contribute to location errors relative to the workpiece. In order to measure the geometrical error caused by motion control and control software and to distinguish from errors explained by other error origins, different feed speeds are applied for the same motion path [18].

Another approach, in order to reduce errors, is to compensate the error based on a previously developed model. Eskandari et al. [22] used a tool path modification in order to compensate for the position error, geometric error and thermal error through different techniques such as regression, neural networks, and fuzzy logic. On the other hand, Fan et al. [23] investigated an error model determined by orthogonal polynomials in an attempt to obtain higher accuracy.

After reviewing the literature, there are several works pertaining to evaluating the performance of machine-tool motion accuracy on a macro-scale but there is no research at all into the characterization of the radial error using a CNC machine in micro-milling processes. This paper provides the insight needed to improve milling as a micro-manufacturing process, by considering the geometrical error caused by motion control and control software error sources when a CNC machining centre or an in-house micro machine centre is used instead of a specialized machine. It is highly useful to characterize machine-tool motion accuracy and evaluate their influence on the desired dimensions and geometrical features of the final piece. Additionally, this will help identify those process parameters — axial depth of cut per pass (ap) and feed per tooth (fz),— which have a greater effect on the ensuing feature quality and to what degree changing these process parameters will affect feature quality. Therefore, this work based on the principles of kinematics, will contribute to understanding the relationship between machine dynamics, process parameters and the quality of the geometrical features on the final micro features. This study is performed without the support of an extra controller, e.g. Aerotech, thus allowing the dynamics of the system to be able to be adjusted online in order to improve the performance of the machine tool. In contrast, an experimental methodology, as an alternative to expensive commercial solutions, is proposed to identify the motion error.

The paper is set out as follows. In Section 2, a brief study of the theoretical principles applied to the milling centre machine used in this work is presented. According to these results, an experimental work is proposed to prove that the contour error in microcavities is mainly affected by the structure and inertia of the machine tool, and that these also produce additional errors as a result of instabilities in the motion control and control software. Section 3 shows the experimental set-up carried out in this work. Furthermore, the process parameters tested allow us to analyze which of them significantly affect accuracy and final shape. The main findings, presented in Section 4, are found through practical methodology and not an expensive commercial solution. Finally, conclusions are presented in Section 5.

2. *Positioning errors due to axis motion*

In the following an attempt to establish the theoretical principles that characterize the CNC machining centre used in this research is made, all the time emphasizing that it is not a specialized machine for micro-milling. In the first part of this section, the structure of the machine is introduced in order to determine the possible kinematic and load errors it may cause. Then a simple model for a circular contouring system is presented with the aim of calculating the error generated by the control motion and control software.

The first consideration to take into account is the difference in the motor type on each axis. In this case, the CNC milling centre used is a Deckel Maho 64V in which the X-axis has a linear motor, whereas the Y-axis has a servomotor which, according with the machine manufacturer, has a positioning precision of 8 and 20 μm, respectively. The configuration of these actuators used on the feed axes is different and crucial to obtaining accuracy in the final pieces. A linear motor has as its base element a moving coil, with 3-phase winding, and a stationary magnet track. Mounted side by side of these is the reactive part of the motor consisting of a steel base with permanently attached magnets (Figure 1a). On the other hand, the rotary servomotor has two principal parts; the stationary stator and the inside rotor (Figure 1b).
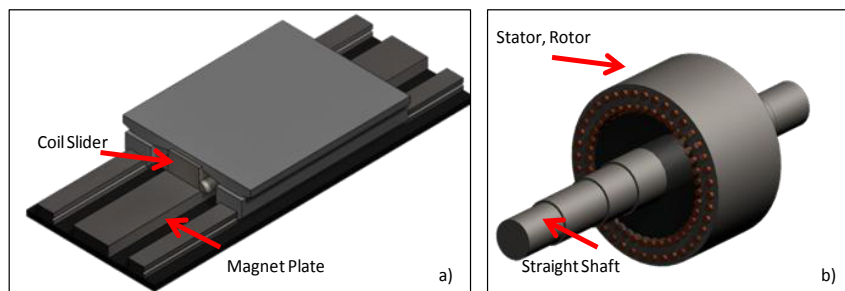

Figure 1 a) Linear Motor in X-axis. b) Servo Motor in Y-Axis.

Some advantages of the linear motor over the servomotor include the elimination of the mechanical actuation assembly. This allows the linear motor to reach higher maximum traverse speeds than the servomotor as the servomotor is limited by its components (ballscrew, leadscrews, ballnuts, gearboxes, etc). In this case, the linear motor has a maximum traverse speed of 70 m/min, while the servomotor drives up to 40 m/min. As for acceleration,

significant inertia of each rotating element in the servomotor is not available in a lineal motor type. Although the linear motor can provide a linear motion system with distinct advantages, thanks to the direct coupling, it is considerably more sensitive to differences in load application. The following equations compare the total inertia of both systems:

The inertia of a rotary system is given as:

$$J_{total} = J_{motor} + J_{ball\ screw} + J_{load}\ [Kg \cdot m^2] \tag{1}$$

The ball screw inertia is calculated as a cylindrical object, according to the following equation:

$$J_{ball\ screw} = \frac{\pi \gamma_b}{32} D_b^4 L_b\ [Kg \cdot m^2] \tag{2}$$

where, γ_b is the weight of the shaft per unit volume, D_b is the shaft diameter and L_b is the shaft length.

For a load moving along a straight line the inertia is:

$$J_{load} = M_{carriage} \left(\frac{l}{2\pi}\right)^2 [Kg \cdot m^2] \tag{3}$$

where, *M carriage* includes all traversing mass and *l* is the travelling distance along a straight line per revolution of the motor.

The assumed specifications of the ball screw, mass of carriage (table and other components) and travelling distance are:

γ_b=7.8X10^3 [Kgm^3]

D_b = 40x10^{-3} [m]

L_b = 1 [m]

M carriage = 650 [Kg]

l = 0.020 [m]

According to manufacturer specifications, motor inertia is 0.0068 Kgm^2, therefore from equation.1; J_{total} is 0.01535 [kg·m^2]

In both cases, the servomotor and linear motor, *M carriage* includes all traversing mass, such as workpiece, bearings, coil slider, encoders, etc. However, according to Equation 3, the *M carriage* is reduced by the second term squared, related to the pitch of the actuator.

In comparison, the load in a linear motor system is the sum of all weights directly connected to the moving coil slider according to Equation 4:

$$M_{total} = M_{coil} + M_{carriage} \ [Kg] \tag{4}$$

Figure 2 shows both carriages on the X and Y-axis. In order to approximate the weight of the carriage on the X-axis the following elements are taken into account: X-axis carriage structure assembly, spindle motor, heat exchanger unit, the tool's cooling system , the spindle traverse carriage (headstock and headstock support, lineal guides) and others (cable hangers, spacers, fixing attachments, etc).
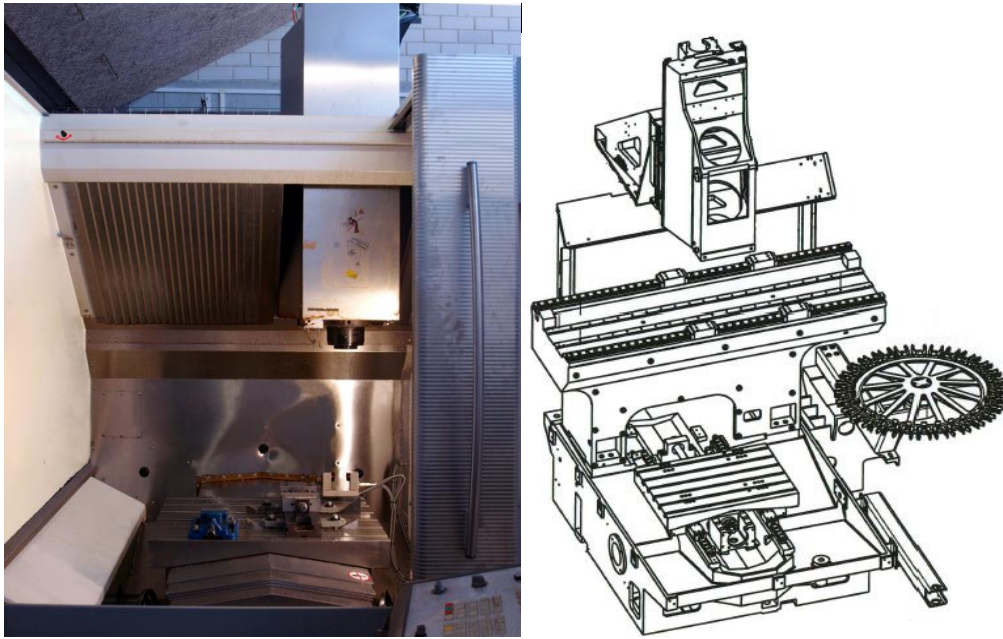

Figure 2 X and Y Axis carriage assembly.

As a result, the translating mass on the X-axis carriage is greater than that on the Y-axis carriage, and consequently, control loop sensitivity to load mass in the X-axis is also greater. This means an additional demand on the controller, in order to maintain performance and stability due to the difference of loads. The contour error for the microcavities is also affected by the servo feedback delay. According to Aun-Neow Poo et al. [24], the simple system model for circular contouring system is given by:

The closed-loop transfer function for this system is:

$$\frac{X_o(s)}{X_i(s)} = \frac{K_x}{s + K_x} \tag{5}$$

$$\frac{Y_o(s)}{Y_i(s)} = \frac{K_y}{s + K_y} \tag{6}$$

Where, X_i, X_0, Y_i, and Y_0 are the Laplace transform of x_i, x_0, y_i and y_0, respectively, K_x and K_y are the X-axis and Y-axis velocity gain, respectively. The system inputs for the circular contour are:

$$x_0 = \frac{K_x R}{\sqrt{K_x^2 + \omega^2}} \sin(\omega t + \alpha_x) + \frac{K_x R \omega}{K_x^2 + \omega^2} e - K_x t \qquad (7)$$

$$y_0 = \frac{K_y R}{\sqrt{K_y^2 + \omega^2}} \cos(\omega t + \alpha_y) + \frac{R \omega^2}{K_y^2 + \omega^2} e - K_y t \qquad (8)$$

Where, R is the radius of the circle and:

$$\alpha_x = \tan^{-1}\left(\frac{-\omega}{K_x}\right) \qquad (9)$$

$$\alpha_y = \tan^{-1}\left(\frac{-\omega}{K_y}\right) \qquad (10)$$

The radial error $e_r(t)$ is given as:

$$e_r(t) = R - \sqrt{x_0^2(t) + y_0^2(t)} \qquad (11)$$

The amount of mismatching in the system velocity gains K_x and K_y is calculated by:

$$\Delta K = K_x - K_y \qquad (12)$$

$$K = \frac{1}{2}\left(K_x - K_y\right) \qquad (13)$$

In order to demonstrate the contour error captured when axes have different dynamic characteristics, the ideal case is shown first. When the system obtains matched gain, the dynamic contour error obtained is very small and in macro machining it is negligible.

Evaluated range for this function is 0-360 degrees but error is defined in Equation 11 as time function. Based on this analysis, it is more useful to depict results in degrees and not in time; hence the maximum value of time is calculated based on the angular velocity in order to evaluate the function from 0 to 2π radians. Figure 3 shows that when the gain mismatch increases in response the radial error also increases.

A useful accuracy indicator of a given function or process is the sum of the predictive quadratic error, which is defined as:

$$J(\theta) = \sum_{m=k}^{n} e_r(k)^2 \qquad (14)$$

Figure 4 shows the sum of square errors and it is evident the growing trend means that when the speed gains are different then one of the axes is moving faster than the other.

However, Figure 5 shows the position of $x_0(t)$ and $y_0(t)$ for all cases and because errors in the cutter path of the circle are small but do exist (in the order of 10^{-3} of R) they cannot be observed by mere sight. In order to obtain a representation of the experimental results, the systems were modelled with a 20 to 1 proportion in the velocity gains (Y axis gain is 20 times

greater than X axis gain, hence the X axis is slower in time response than the Y axis). Figure 6 shows that when the difference in the velocity gains is magnified, the contour error for circle generation is significant. Note that the drive element friction effects have not been considered and that the model was simplified; although these can be taken into account in future work.
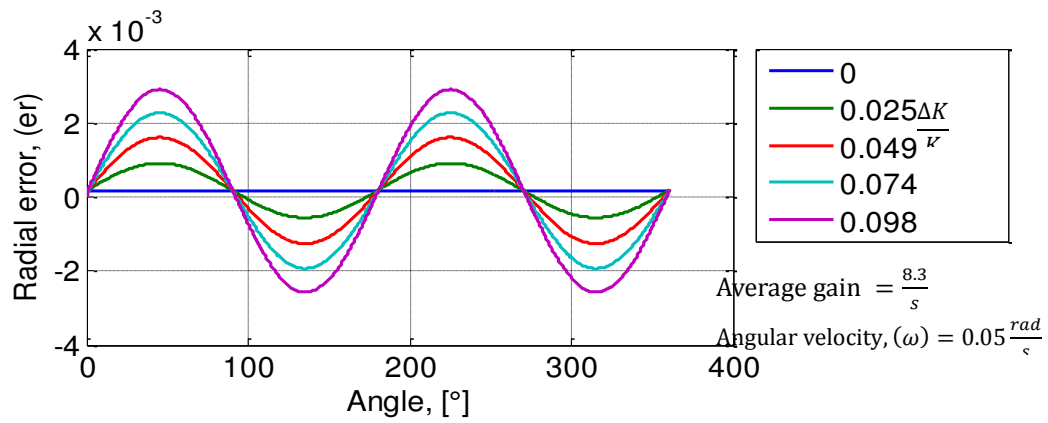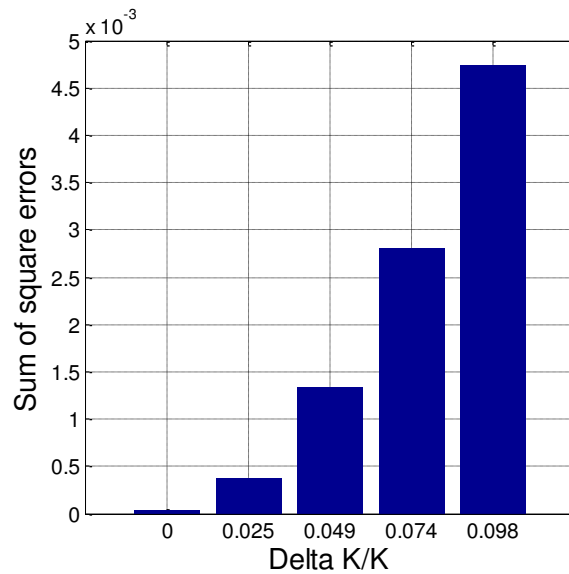

Figure 3 Radial error obtained with mismatched gains.
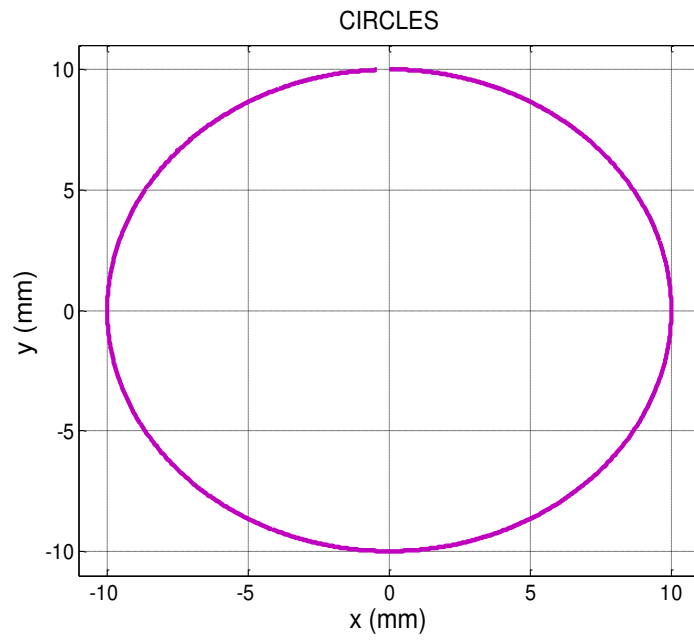

Figure 4 Sum of square errors.

CIRCLES

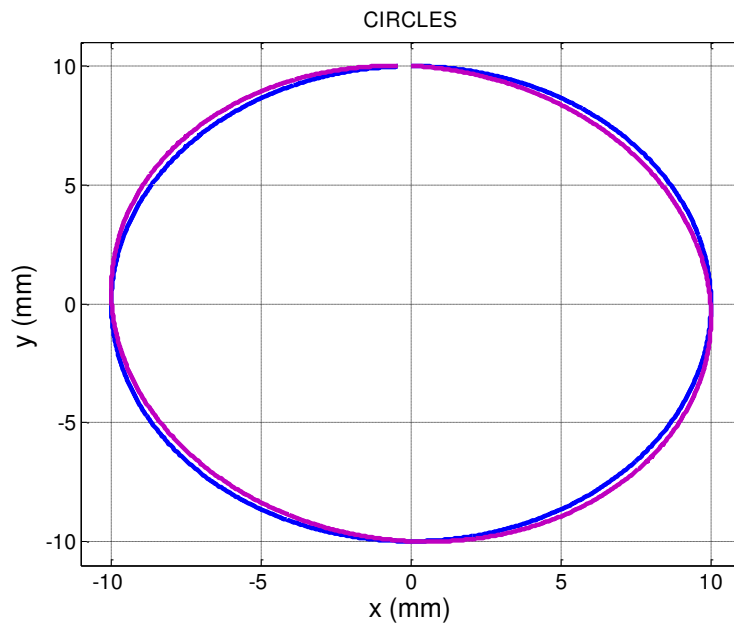Figure 5 Circle trace for mismatched gains.

CIRCLES

Figure 6 Circle trace for magnified mismatched gains.

3. *Experimental set-up*

The CNC milling machine used to perform the experiment was a Deckel-Maho[©] 64V Linear (3-axis, vertical spindle) with a positioning accuracy of 20 and 10 μm in Y and Z directions, respectively and 8 μm in X direction. The machine centre has a speed ranging from 1 to 12,000 rpm and is driven by a 19KW spindle drive motor. The FANUC 180i controller offers control of up to three independent part program paths with up to eight servo-controlled axes per path at increments as low as 0.1 μm. To minimize errors, heat-shrink tool holders and an EROWA©

clamping system were used in all the experiments. Figure 7 provides a close-up view of the machining set-up. Furthermore, a warm-up was performed in order to preserve the thermal conditions and avoid producing any thermo-mechanical errors.
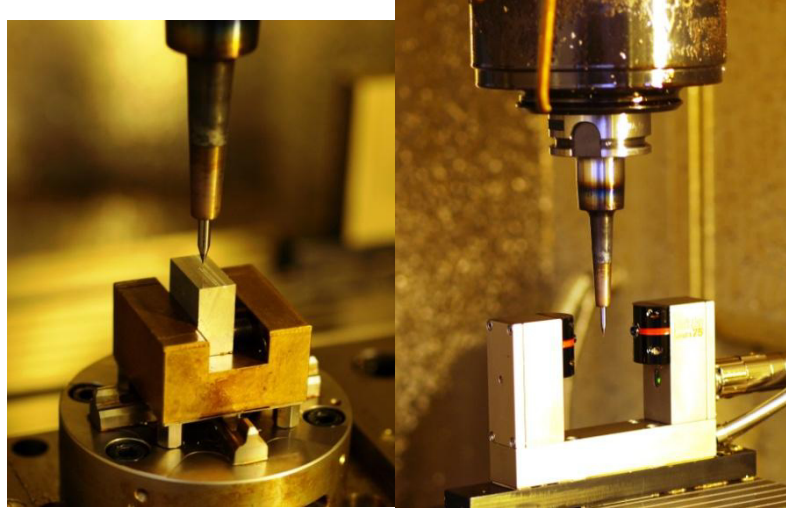

Figure 7 Left: Tool, tool holder, and EROWA© clamping system set-up. Right: Mida Laser Line©.

The workpiece material tested in this study was aluminum alloy (Al 7075-T6) with a hardness of 90 HRB due to its high machinability. Test blocks of dimensions 12x25x25 mm were prepared as a raw material. A Mitsubishi© MS2SBR0010S04 ball nose end mill tool of 200 μm in diameter was used. Figure 8 and Table 1 show the geometric characteristics of the tools. Before performing the milling operations, the micro-tool was measured with a Non-contact Laser System supplied by Mida© (repeatability of $2\sigma \leq 0.2$ μm) in order to compensate for tool errors (Figure 7 right). A conventional mineral-oil coolant was used (CUTTINSOL 5 by COLGESA©). Experiments were carried out by machining micro-elliptical cavities of 525 μm on the major axis, 500 diameter μm on the minor axis and 250 μm in depth, as Figure 9 shows. This geometry was selected in order to enhance the effect of the differences between the X-axis motion and Y-axis motion.
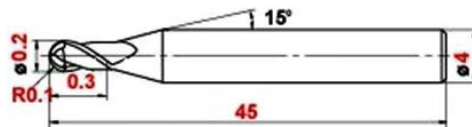

Figure 8 Mitsubishi MS2SBR0010S04 ball nose end mill schematically represented.

Table 1. Geometric characteristics of the ball nose end mill cutter.

Coating	MS: (Al, Ti)N
Tool Interference Corner (B2) [°]	15
Cutting Diameter (D1) [mm]	0.2
Shank Diameter (D4) [mm]	4

Overall Length (L1) [mm]	45
Length of Cut (ap) [mm]	0.3
Number of flutes	2

Table 2 shows the factors analyzed. Experimental design was defined by three factors: axial depth of cut per pass (ap), feed per tooth (fz), and axis machining direction. The X-Axis machining direction is defined when all micro-cavities are aligned along the X direction, as shown in Figure 9, while the Y-Axis machining direction is when cavities are aligned through the Y axis machine direction. Response variables related to accuracy were divided into two desired dimensions: (major axis (M) and minor axis (m), (see Figure 9). Micro-cavity shape was also evaluated.

Dimensional measurements on the XY plane were performed with a Microscope Discovery 12 from Zeiss© and Quartz PCI© Software was used to collect the digital images (150x magnification).

Table 2. Variable factors and factor levels performed.

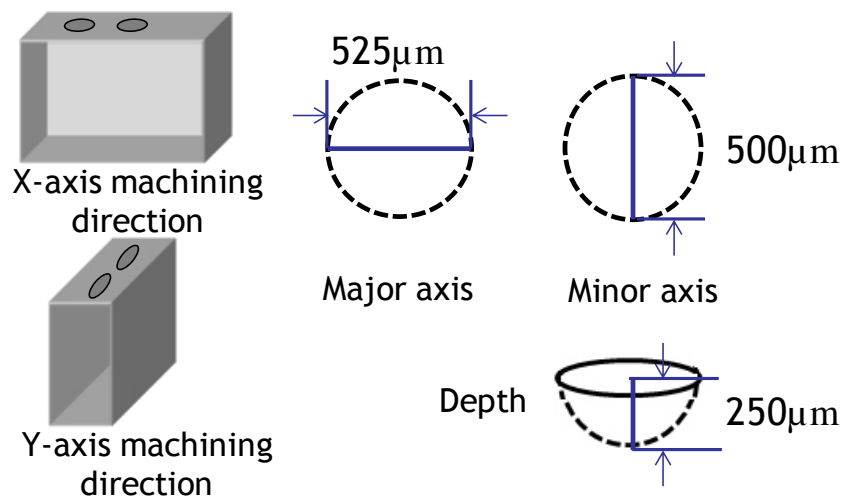| Variable Factors	Factor Levels			
F1. Axial depth of cut per pass ap,(μm)	2.0	2.25	2.50	3.0
F2. Feed per tooth fz, (μm/tooth)	3.30		4.95	
F3. Axis machining 0=X-axis, 1=Y-axis	0		1	

Figure 9 Sectional view and desired dimensions of micro-cavity (without scale).

4. Results and discussion

Table 3 shows three different inputs, such as axial depth of cut per pass, feed per tooth and axis machining direction for experimental sets and two measured outputs on the shape machined i.e. major axis and minor axis. In addition, relative errors were calculated using desired measures and those measures obtained. The maximum error obtained when X-axis direction machining is used is 12%, while in the Y-axis direction the maximum error is of 3.65%. Minimum error results are 1.4 and 0.6, respectively. According to these results, it may be possible to develop a compensation model in simple geometries, such as microcavities, and a practical solution could be used to compensate the desired profile in the CAD program and then generate the part machining program.

Table 3. Experimental results.

Test	Axial depth of cut per Pass a_p [µm]	Feed per Tooth f_z [µm/z]	Axis machining *0=X *1=Y	Major Axis M [µm]	Minor Axis M [µm]	Major Axis Error εØX [±%]	Minor Axis Error εØY [±%]	Test	Axial depth of cut per Pass Ap [µm]	Feed per Tooth fz [µm/z]	Axis machining *0=X *1=Y	Major Axis M [µm]	Minor Axis m [µm]	Major Axis Error εØX [±%]	Minor Axis Error εØY [±%]
1	3.00	3.30	0	550	518	4.76	3.60	25	3.00	3.30	1	539	508	2.67	1.60
2	3.00	3.30	0	548	560	4.38	12.00	26	3.00	3.30	1	540	507	2.86	1.40
3	3.00	3.30	0	550	513	4.76	2.60	27	3.00	3.30	1	543	510	3.43	2.00
4	2.50	3.30	0	548	518	4.38	3.60	28	2.50	3.30	1	538	505	2.48	1.00
5	2.50	3.30	0	541	513	3.05	2.60	29	2.50	3.30	1	540	506	2.86	1.20
6	2.50	3.30	0	550	520	4.76	4.00	30	2.50	3.30	1	537	503	2.29	0.60
7	2.25	3.30	0	553	523	5.33	4.60	31	2.25	3.30	1	544	512	3.62	2.40
8	2.25	3.30	0	543	512	3.43	2.40	32	2.25	3.30	1	537	510	2.29	2.00
9	2.25	3.30	0	540	518	2.86	3.60	33	2.25	3.30	1	543	503	3.43	0.60
10	2.00	3.30	0	553	522	5.33	4.40	34	2.00	3.30	1	541	505	3.05	1.00
11	2.00	3.30	0	543	532	3.43	6.40	35	2.00	3.30	1	542	536	3.24	7.20
12	2.00	3.30	0	542	518	3.24	3.60	36	2.00	3.30	1	537	512	2.29	2.40
13	3.00	4.95	0	544	519	3.62	3.80	37	3.00	4.95	1	546	511	4.00	2.20
14	3.00	4.95	0	552	514	5.14	2.80	38	3.00	4.95	1	557	509	6.10	1.80
15	3.00	4.95	0	549	507	4.57	1.40	39	3.00	4.95	1	552	516	5.14	3.20

16	2.50	4.95	0	558	521	6.29	4.20	40	2.50	4.95	1	545	511	3.81	2.20
17	2.50	4.95	0	553	515	5.33	3.00	41	2.50	4.95	1	554	513	5.52	2.60
18	2.50	4.95	0	550	508	4.76	1.60	42	2.50	4.95	1	545	507	3.81	1.40
19	2.25	4.95	0	549	522	4.57	4.40	43	2.25	4.95	1	544	519	3.62	3.80
20	2.25	4.95	0	551	513	4.95	2.60	44	2.25	4.95	1	520	549	0.95	9.80
21	2.25	4.95	0	548	507	4.38	1.40	45	2.25	4.95	1	548	515	4.38	3.00
22	2.00	4.95	0	551	520	4.95	4.00	46	2.00	4.95	1	557	517	6.10	3.40
23	2.00	4.95	0	551	527	4.95	5.40	47	2.00	4.95	1	552	534	5.14	6.80
24	2.00	4.95	0	548	507	4.38	1.40	48	2.00	4.95	1	548	514	4.38	2.80

An in-depth analysis of the major axis (M) measure was conducted. Table 4 summarizes the results of the ANOVA analysis. Table 4 reveals that feed per tooth and the machining axis are the most significant factors in the major axis (M) measure. This confirms that the geometrical error sources are motion control and control software and can be identified by, as mentioned in Section 1, applying different feeds for the same motion path [18].

Table 4. ANNOVA for major axis (M) measure

Factor	D.F.	SC Sec.	SC ajust.	Mc ajust	F	P
Axial depth of cut per pass	3	129.75	129.75	43.25	1.30	0.286
Feed per Tooth	1	352.08	352.08	352.08	10.60	0.002
Axis machining	1	280.33	280.33	280.33	8.44	0.006
Error	42	1395.08	1395.08	33.22		
Total	47	2157.25				

Figure 10 shows the main effects plots on the major axis (M) measure. When feed per tooth increases, the major axis (M) also increases. On the other hand, when x-axis machining is used the major axis (M) measure is greater than when y-axis machining is used.
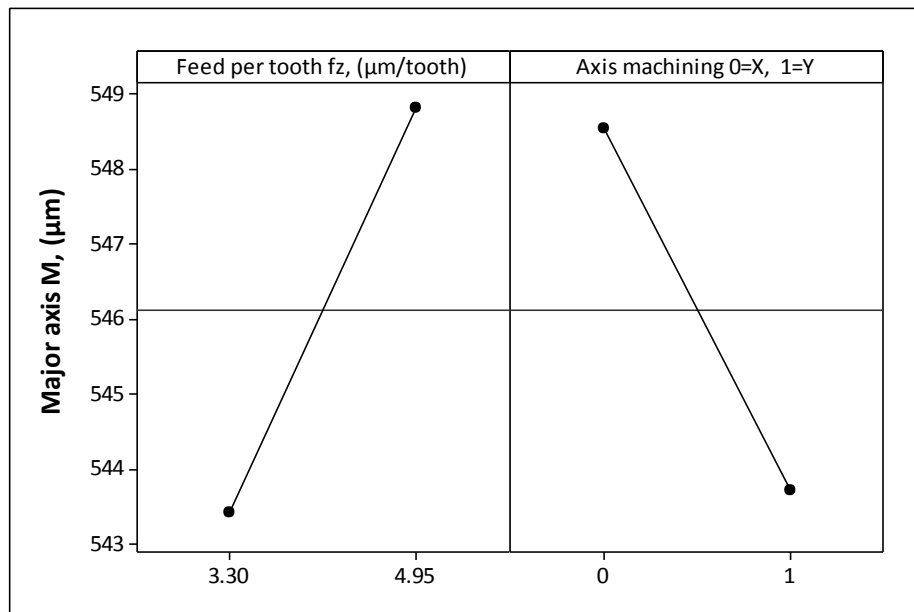
Figure 10 Main effects plot for major axis (M) measure

Figure 11 shows that the values of major (M) and minor axis (m) exceed the desired value of 525μm and 500 μm, respectively. When both graphics are compared, it is evident that the values of the major and minor axes on the X-axis machining direction are larger than the values obtained on the Y-axis machining direction. Figure 12 shows a micro-cavity in the XY plane. It is also worth mentioning that when the axis of machining is the X-axis, the value of the major axis is greater than the value obtained using the Y-axis machining direction. So, and according to the results, it can be concluded that the difference between the X-axis motion and Y-axis motion is what is affecting the accuracy of the final shape.
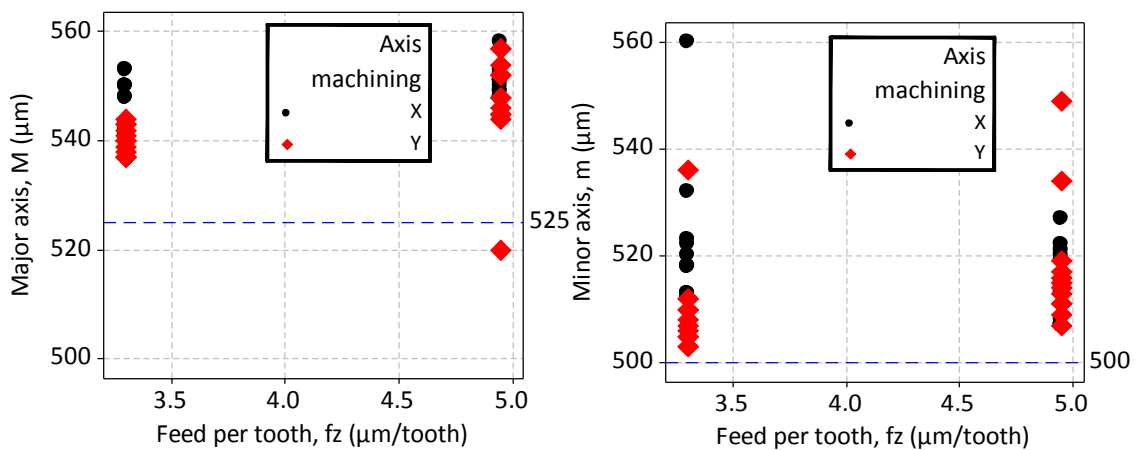

Figure 11 Effect of feed per tooth using X and Y axes machining directions on major and minor axes.
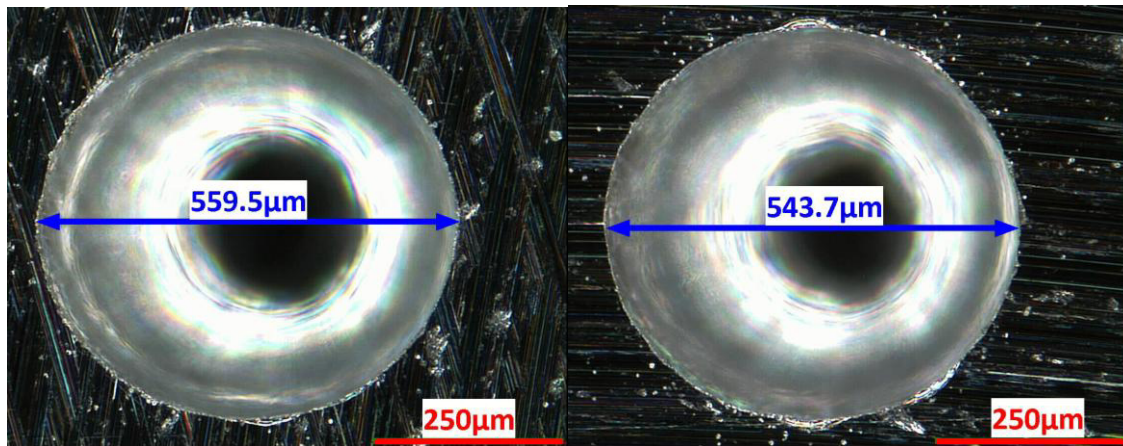
Figure 12 Measure of the major axis (M) a) Micro-cavity performed using X-axis machining (left) and performed using Y-axis machining (right).

These results can be explained by machine kinematics. Figure 13 shows a schematic explanation for the tendency of the ellipses long axes. A spindle motor starts with an initial speed to go from point A to point B, using the path in double line. When the micro-tool arrives at point B, the spindle motor decelerates in order to end at zero speed, however, when working with micro distances another trajectory is machined (triple line) because of the inertia of the spindle and consequently this fails to stop as desired. On a macro-scale, these accelerations and decelerations are not as noticeable because these variations, compared with the dimensional size of the pieces are negligible, but on a micro-scale they are proportionally important. The explanation for this behaviour is that, as distances are short the programmed feed rate is never reached.
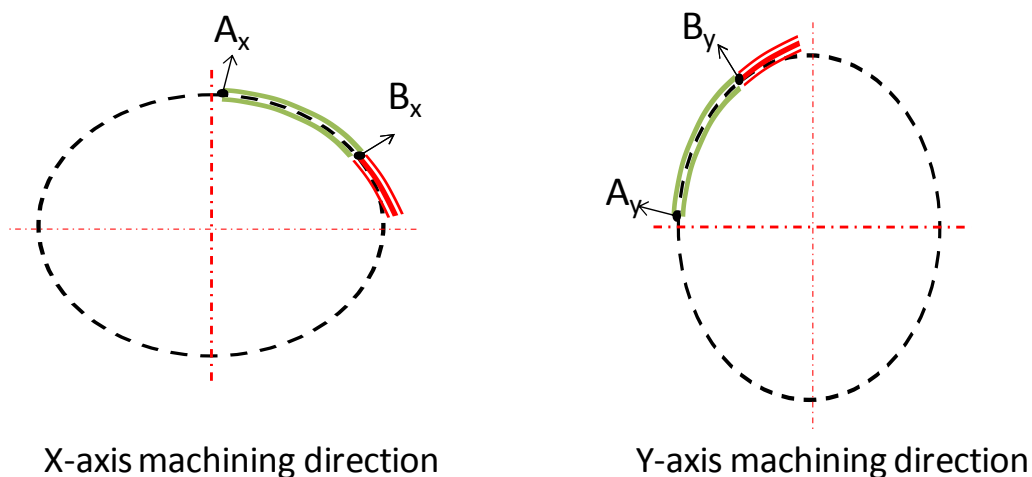

X-axis machining direction   Y-axis machining direction

Figure 13 Schematic view of Acceleration/Deceleration effect on the trajectory of the micro tool.

The results obtained by the calculated relative errors infer that the influence of acceleration and deceleration is not the only element that affects the accuracy of the final feature. Figure 14 shows that the errors obtained are not equal when an X-axis direction is used or when a Y-axis machining direction movement is used. The graphics demonstrate that the percentage

errors on both axes of the ellipse (major and minor axes) are lowest when it is machined in the Y-axis direction. The results show that the geometrical error is caused mainly by three sources; all of which are related to each other. The kinematic errors caused by the machine's structure and because there are not the same loads in the moving carriages, produce motion control and control software errors.
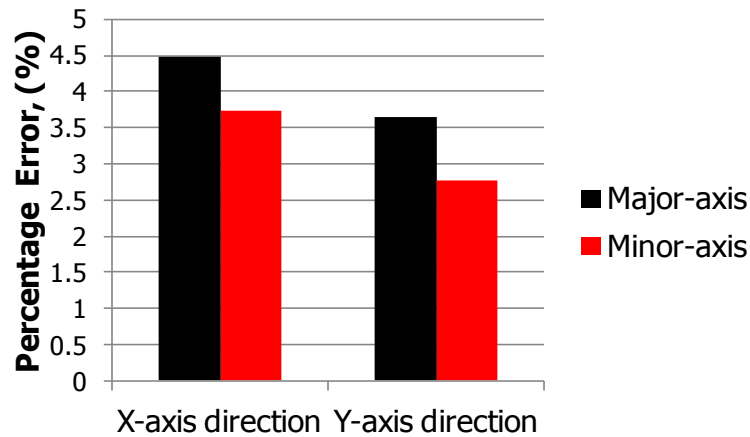

Figure 14 Dimensional errors according to the axis of machining.

According to experimental data by Andolfatto et al. [25], the repartition of the mean value of the error sources along the experimental trajectory, on a macro-scale, are shown in Table 5. The major source of error is the link errors at 86.9%. Table 5 also shows the percentages applied to the mean values of the experimental data in this work. The comparison is made in order to emphasize that while on a macro-scale the errors may be negligible, on a micro-scale it means that the manufactured final product does not comply with the desired dimensions. In addition, the most influential factor on the geometrical error are the link errors and on average these errors affect the end product with 86.9% of the total error. In comparison with some previous research by Chen et al. [3], these authors used a three-axis CNC horizontal machining centre and developed a displacement measurement approach. They found that one of the maximum translational errors is 29 microns. This is evidence that, although on a macro-scale this is insignificant, on a micro-scale this has an enormous affect because the characteristics of the final piece contain details of the same size. Moreover, the Andolfatto et al. [25] study quantifies the dynamic errors as 0.6%, but on a micro-scale this error increases as a result of micro tool deflections and vibrations. Thus, further research should be performed in order to analyze this error source.

Table 5 Repartition of the mean value of the error sources (Adapted from Andolfatto et al. [2011]) and applied to the experimental data of this work.

			x-axis direction		y-axis direction	
			Major axis	Minor axis	Major axis	Minor axis
Error sources		%	[μm]	[μm]	[μm]	[μm]
Contouring errors		1.1	0.259	0.110	0.210	0.163
Quasi-static geometric errors	Link errors	86.9	20.458	8.726	16.620	12.890
	Motion errors	11.4	2.684	1.145	2.180	1.691
	Thermal drift	0	0	0	0	0
Dynamic errors		0.6	0.141	0.060	0.115	0.089

5. Conclusions

This work investigates the machine-tool motion accuracy of a medium CNC machine in the micro-milling of elliptical cavities. Furthermore, it studies the influence of the process parameters and the quality of the geometrical features on the final micro shape features. The methodology of this study includes an analysis of the structure of the machine which used in the tests, as well as a model to test the control motion and control software. Then, an experimental study was performed with a geometry selected to evaluate the error which is produced according to the theoretical principles studied. Furthermore, a brief comparison of the results with previous studies on a macro-scale has been incorporated.

Some specific conclusions can be drawn as follows:

- The present work developed an experimental approach in order to characterize the radial error using a CNC machine instead of specialized machine or in-house micro machine centre in the micro-milling process. Furthermore, this methodology is a practical solution replacing expensive commercial solutions such as laser interferometer, double ball bar, laser Doppler vibrometers, etc.

- Results suggest that CNC standard machine tools are capable of performing micro-milling to produce micro-cavities, but inertial and kinematic values are highly significant when it comes to affecting motion control.

- The dimensions of the cavities obtained were close to the desired values; achieving a percentage of error below 5%.

- It could be seen that, by performing an inspection of the machine tool, the mass moved by the X-axis is greater than the mass moved by the Y-axis. Mass has a direct effect on inertial force thus, the greater the mass, the slower the time response of the system, because X-axis mass is greater than Y-axis mass and this results in a greater error in the X-axis. Experimental results confirm that the difference in axes' motion produces errors in the final micro part. Using a medium milling centre with similar characteristics for micro-milling could be proposed a compensation model.

- Accuracy and final shape are affected by the dynamics of machine tool. At a micro-scale, accelerations and decelerations are significant and cannot be assumed to be negligible, as they would be in the case of macro-scale. Results suggest that accuracy and final shape are mainly influenced by feed per tooth.

References

[1] Weck, M., Schmidt, M. (1986). A new method for determining geometric accuracy in the axis of movement of machine tools. Precision Engineering, 8(2): 97-103.

[2] Zhang, G., Ouyang, R., Lu, B., Hocken, R., Veale, R., Donmez, A. (1988). A displacement method for machine geometry calibration. CIRP Annals-Manufacturing Technology, 37(1): 515-518.

[3] Chen, G., Yuan, J., Ni, J. (2001). A displacement measurement approach for machine geometric error assessment. International Journal of Machine Tools and Manufacture, 41(1): 149-161.

[4] Iwasawa, K., Iwama, A., Mitsui, K. (2004). Development of a measuring method for several types of programmed tool paths for NC machine tools using a laser displacement interferometer and a rotary encoder. Precision engineering, 28(4): 399-408.

[5] Bryan, J. B. (1982). A simple method for testing measuring machines and machine tools Part 1: Principles and applications. Precision Engineering, 4(2): 61-69.

[6] Kakino, Y., Ihara, Y., Nakatsu, Y., Okamura, K. (1987). The measurement of motion errors of NC machine tools and diagnosis of their origins by using telescoping magnetic ball bar method. CIRP Annals-Manufacturing Technology, 36(1: 377-380.

[7] Lai, J. M., Liao, J. S., Chieng, W. H. (1997). Modeling and analysis of nonlinear guideway for double-ball bar (DBB) measurement and diagnosis. International Journal of Machine Tools and Manufacture, 37(5): 687-707.

[8] Qiu, H., Li, Y., Li, Y. (2001). A new method and device for motion accuracy measurement of NC machine tools. Part 1: principle and equipment. International Journal of Machine Tools and Manufacture, 41(4): 521-534.

[9] Qiu, H., Li, Y., & Li, Y. (2001). A new method and device for motion accuracy measurement of NC machine tools. Part 2: device error identification and trajectory measurement of general planar motions. International Journal of Machine Tools and Manufacture, 41(4), 535-554.

[10] Schmitz, T. L., Ziegert, J. C., Canning, J. S., Zapata, R. (2008). Case study: A comparison of error sources in high-speed milling. Precision Engineering, 32(2): 126-133.

[11] Rehsteiner, F., Weikert, S., IWF, E. (1996). Analysis of tool trajectories (2D tool paths) in machine tools. In Proceedings of the ASPE 1996 Annual Meeting, Monterey, Calif., Nov (pp. 4-19).

[12] Du, Z., Zhang, S., Hong, M. (2010). Development of a multi-step measuring method for motion accuracy of NC machine tools based on cross grid encoder. International Journal of Machine Tools and Manufacture, 50(3): 270-280.

[13] Kim, D. I., Song, J. I., & Kim, S. (1994, October). Dependence of machining accuracy on acceleration/deceleration and interpolation methods in CNC machine tools. In Industry Applications Society Annual Meeting, 1994., Conference Record of the 1994 IEEE (pp. 1898-1905). IEEE.

[14] Monreal, M., Rodriguez, C. A. (2003). Influence of tool path strategy on the cycle time of high-speed milling. Computer-Aided Design, 35(4): 395-401.

[15] Schmitz, T. L., Ziegert, J. C., Canning, J. S., Zapata, R. (2008). Case study: A comparison of error sources in high-speed milling. Precision Engineering, 32(2): 126-133.

[16] Phillip, A. G., Kapoor, S. G., DeVor, R. E. (2006). A new acceleration-based methodology for micro/meso-scale machine tool performance evaluation. International Journal of Machine Tools and Manufacture, 46(12): 1435-1444.

[17] Anandan, K. P., Tulsian, A. S., Donmez, A., Ozdoganlar, O. B. (2012). A Technique for measuring radial error motions of ultra-high-speed miniature spindles used for micro-machining. Precision Engineering, 36(1): 104-120.

[18] Schwenke, H., Knapp, W., Haitjema, H., Weckenmann, A., Schmitt, R., Delbressine, F. (2008). Geometric error measurement and compensation of machines—an update. CIRP Annals-Manufacturing Technology, 57(2): 660-675.

[19] Gomez-Acedo, E., Olarra, A., de la Calle, L. L. (2012). A method for thermal characterization and modeling of large gantry-type machine tools. The International Journal of Advanced Manufacturing Technology, 62(9-12): 875-886.

[20] Liu, Y., Lu, Y., Gao, D., Hao, Z. (2013). Thermally induced volumetric error modeling based on thermal drift and its compensation in Z-axis. The International Journal of Advanced Manufacturing Technology, 69(9-12): 2735-2745.

[21] Lu, Y., Islam, M. N. (2012). A new approach to thermally induced volumetric error compensation. The International Journal of Advanced Manufacturing Technology, 62(9-12): 1071-1085.

[22] Eskandari, Sina, Behrooz Arezoo, Amir Abdullah. (2013) Positional, geometrical, and thermal errors compensation by tool path modification using three methods of regression, neural networks, and fuzzy logic. The International Journal of Advanced Manufacturing Technology, 65 (9-12):. 1635-1649.

[23] Fan, Kaiguo, Jianguo Yang, Liyan Yang. (2013) Orthogonal polynomials-based thermally induced spindle and geometric error modeling and compensation. The International Journal of Advanced Manufacturing Technology, 65 (9-12): 1791-1800

[24] Poo, A. N., Bollinger, J. G., & Younkin, G. W. (1972). Dynamic errors in type 1 contouring systems. Industry Applications, IEEE Transactions on, (4): 477-484.

[25] Andolfatto, L., Lavernhe, S., Mayer, J. R. R. (2011). Evaluation of servo, geometric and dynamic error sources on five-axis high-speed machine tool. International Journal of Machine Tools and Manufacture, 51(10): 787-796.